

Supplemental Material

A comparison of leak compensation function in acute care ventilators during non-invasive and invasive ventilation; a lung model study

Jun Oto, M.D., PhD, Christopher T. Chenelle, B.A., Andrew D. Marchese, B.S., Robert M Kacmarek PhD, RRT.

Methods

ASL5000 lung model (IngMar Medical; Pittsburgh, PA)¹ is a computerized lung simulator consisting of a piston moving inside a cylinder. Compliance, resistance, and the inspiratory muscle pressure profile (negative pressure created by respiratory muscles) are set by the user.

Each ventilator evaluated was connected to the lung simulator by the manufacturer's standard circuit, if available, or a standard disposable corrugated circuit (Hudson; Temecula, CA). All of the ventilators were studied with a dry circuit; humidifiers and heat and moisture exchanger were removed.

Study setup (ASL5000 interface and Mannequin)

In the non-invasive mode, a mannequin head was used to simulate the patient-mask interface. Endotracheal tubes fitted into the mouth and nostrils directed gas coming from a facemask to the simulator (Figure. 1). These nasal and oral tubes met in a common airway leading to the SBLVM, which then lead to the ASL5000. An oronasal facemask (PerformaTrack SE; Respirationics Inc; Murrysville, PA) was affixed to the head of the mannequin with standard straps.

During invasive ventilation assessment, the ventilators were affixed to the ASL5000 with an 8 mm internal diameter endotracheal tube.

Data collection and analysis

Continuous data from the lung simulator were compared using a Wilcoxon test to assess the impact of leak, different lung mechanics, or PEEP settings on synchronization. Friedman test followed by Bonferroni correction for multiple comparisons was used for overall comparisons between ventilators. Statistical analysis was done with a statistical software package (PASW Statistic 18; SPSS; Chicago, IL). A $p < 0.05$ was considered significant. Regarding the time to baseline pressure, delayed cycling time, and delivered tidal volume, differences greater than 10% were considered important. We report only differences of these parameters that were both statistically significant and important because of the small standard deviations observed with lung model studies, which result in differences being statistically significant even when within measurement error.

Additional results

Synchronization

In non-invasive mode, the Servo I, the PB840, the C3, and the V60 synchronized to all increasing and decreasing leaks in both COPD and ARDS models for all scenarios. The G5 could not synchronize to leaks L2 and L3 under PEEP 10 cmH₂O in both COPD and ARDS models. The CareStation and the V500 could not synchronize to leaks L2 and L3 in both PEEP settings. The Avea could not synchronize to all L1 to L3 leak scenarios.

In invasive mode, only the PB840 and the V60 synchronized to all increasing and decreasing leaks in both PSV and PAC for all leak scenarios. The C3, the G5 and the V500 could not synchronize to leaks L3 in both PSV and PAC. The CareStation could not synchronize to leaks L2 and L3 in both PSV and PAC. The Servo I and the Avea could not synchronize to all L1 to L3 leak scenarios.

Increasing leak vs. decreasing leak:

In non-invasive mode, B to synch, miss-triggering, auto-triggering and time to settle were higher for increasing than decreasing leaks (Supple. table 1A). During increasing leak, auto-triggering occurred more frequently than miss-triggering ($p < 0.001$). During decreasing leak, miss-triggering occurred more frequently than

auto-triggering ($p < 0.001$) (Figure 1). As leak gradient increased, B to synchrony, and miss-triggering increased during both increasing and decreasing leak ($p < 0.001$).

In invasive mode, B to synchrony, miss-triggering, auto-triggering and time to settle were higher for increasing than decreasing leaks in both PSV and PAC (Suppl. table 1B). During increasing leak, auto-triggering occurred more frequently than miss-triggering. During decreasing leak, miss-triggering occurred more frequently than auto-triggering in both PSV ($p=0.02$) and PAC ($p=0.01$). As leak gradient increased, B to synchrony, and miss-triggering increased during both increasing and decreasing leak ($p < 0.001$).

PSV vs. PAC:

There were significant differences in B to synchrony, miss-triggering and time to settle between PSV and PAC, with PAC outperforming PSV in all three categories (Suppl. table 3). Auto-triggering did not differ between ventilator modes. The representative waveform of airway pressure for both PSV and PAC are shown in Suppl. Figure 3. In brief, after changing leak, PSV allowed prolonged inspiratory time (delayed cycling), result in miss-triggering at the next breath. On the other hand, PAC has fixed inspiratory time and does not induce trigger asynchrony due to delayed cycling at the next breath.

Triggering pressure and delivered tidal volume

Triggering pressure:

In non-invasive mode, there were no significant differences in the triggering pressure between the COPD model and the ARDS model (-1.9 ± 2.1 cmH₂O vs. -1.5 ± 0.3 cmH₂O, $p=0.21$). The triggering pressure was smallest for the V60 and largest for the Servo-*i* in both the COPD model and the ARDS model ($p < 0.001$).

In invasive mode, there were no significant differences in the triggering pressure between the COPD model and the ARDS model both in PSV (-1.6 ± 0.5 cmH₂O vs. -1.5 ± 0.4 cmH₂O, $p=0.66$) and PAC (-1.6 ± 0.5 cmH₂O vs. -1.5 ± 0.4 cmH₂O, $p=0.66$). The triggering pressure was smaller for the V60 than the PB840 in both COPD and ARDS model ($p < 0.001$).

Tidal volume:

In non-invasive mode, tidal volume was larger in the COPD model than the ARDS model (530 ± 101 ml vs. 281 ± 43 ml, $p < 0.001$). In all ventilators, as leak increased, tidal volume decreased in both the COPD and the ARDS model. The tidal volume was largest for the Servo-*i* and smallest for the C3 (615 ± 85 ml vs. 465 ± 73 ml) in the COPD model and largest for the V60 and smallest for the C3 (307 ± 31 ml vs. 241 ± 46 ml) in the ARDS model.

In invasive mode, tidal volume was larger in COPD model than ARDS model in both PSV (576 ± 90 ml vs. 317 ± 29 ml, $p < 0.001$) and PAC (593 ± 89 ml vs. 324 ± 27 ml, $p < 0.001$). The tidal volume was larger for the PB840 than the V60 in both PSV (606 ± 62 ml vs. 472 ± 60 ml, $p < 0.001$) and in PAC (627 ± 61 ml vs. 489 ± 53 ml, $p < 0.001$), but did not differ in the ARDS model (PSV: 289 ± 26 ml vs. 311 ± 25 ml, $p < 0.001$ but within 10% differences) (PAC: 300 ± 26 ml vs. 311 ± 25 ml, $p = 0.04$, but within 10% differences). There were no significant differences between PSV and PAC in both the COPD model ($p=0.39$) and the ARDS model ($p=0.25$) (Suppl. Figure 7).

Figure legends

Suppl. Figure 1

Illustration of the experimental setup

A) Different ventilators are connected to the mask on the head of the mannequin and deliver air to the ASL5000 lung simulator via the SBLVM during non-invasive ventilation.

B) Different ventilators are connected to the endotracheal tube, internal diameter 8.0 mm, and deliver air to the ASL5000 lung simulator via the SBLVM during invasive ventilation.

SBLVM, simulator bypass and leak valve module

Suppl. Figure 2

Auto- and miss-triggering under increasing and decreasing leak during pressure assist/control ventilation

Miss-triggering:

†, Decreasing leak: L3→B > L1→B ($p < 0.01$), L3→B > L2→B ($p < 0.05$), L3→B > L2→L1 ($p < 0.05$)

Each box represents the inter-quartile range between the 25th and the 75th percentiles, with the median value. Vertical bars represent the maximum and minimum values except for outliers. Outliers identified with a circle are any data values which lie greater than 1.5 times the box length beyond the lower or higher edges of the box and within 3.0 times the box length. Extreme outliers identified with a star are any data which lie more than 3.0 times the box length beyond the lower or higher edges of the box.

PSV, pressure support ventilation; PAC, pressure assist/control ventilation; B to synch, number of breaths to synchronization

Suppl. Figure 3

Representative wave form of PSV and PAC just after changing leak

(A) Representative airway and muscle pressure wave trace in PSV mode. After the changing leak level (L2→L3), auto-triggering (black arrow) occurred and inspiratory time was reached the maximum duration of inspiration setting (1.5 sec), resulting in miss-triggering (gray arrow) at the next breath.

(B) Representative airway and muscle pressure wave trace in PAC mode. After the changing leak level (L2→L3), auto-triggering (black arrow) occurred and inspiratory time was limited the pre-setting inspiratory time (0.9 sec) and does not induce trigger asynchrony at the next breath.

P_{aw} , airway pressure; P_{mus} , muscle pressure

Suppl. Figure 4

Time to baseline pressure under leak scenario in COPD and ARDS models during pressure assist/control ventilation

Absent bars indicate failure to synchronize during the leak scenario. The histogram bars show mean value.

Suppl. Figure 5

Delayed cycling time under leak scenario in COPD and ARDS models during pressure assist/control ventilation. The histogram bars show mean values.

Suppl. Figure 6

Trigger pressure under leak scenario in COPD and ARDS models during pressure assist/control ventilation. The histogram bars show mean values.

Suppl. Figure 7

Delivered tidal volume under leak scenario in COPD and ARDS models during pressure assist/control ventilation. The histogram bars show mean values.

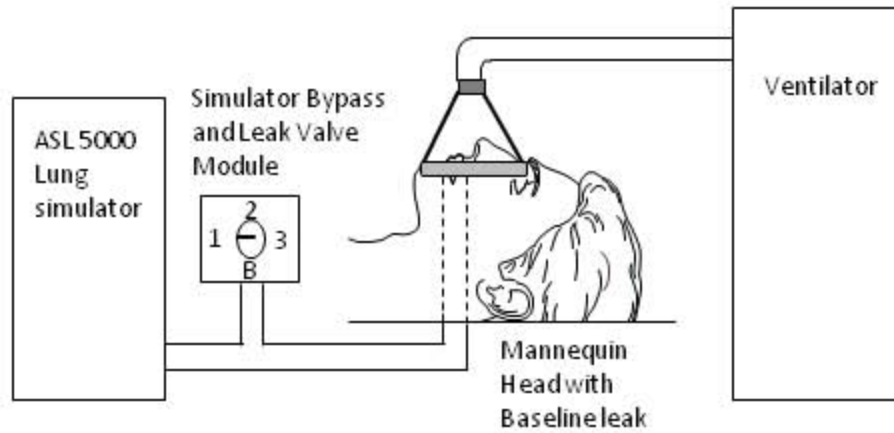
References

1. IngMar Medical. ASL5000 Active Servo Lung Computerized Breathing Simulator and Ventilator Test Instrument user`s manual. Pittsburgh, PA: IngMar Medical, 2006

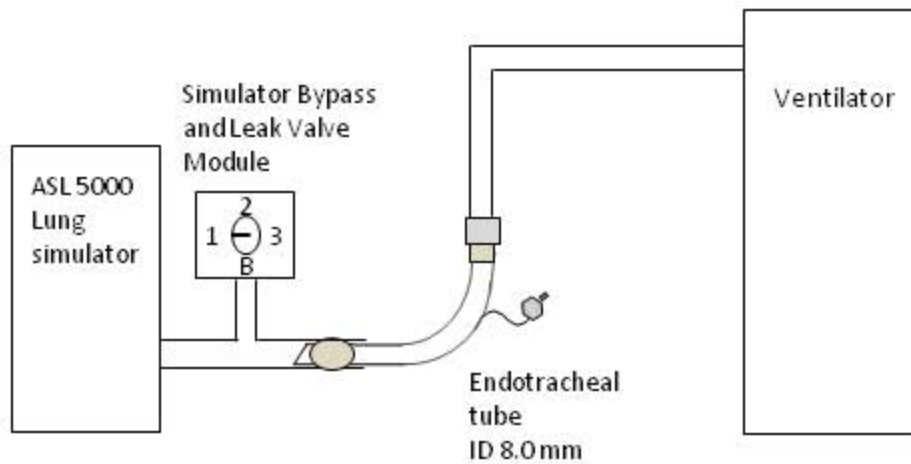
Suppl. Figure. 1

ONLINE DATA SUPPLEMENT

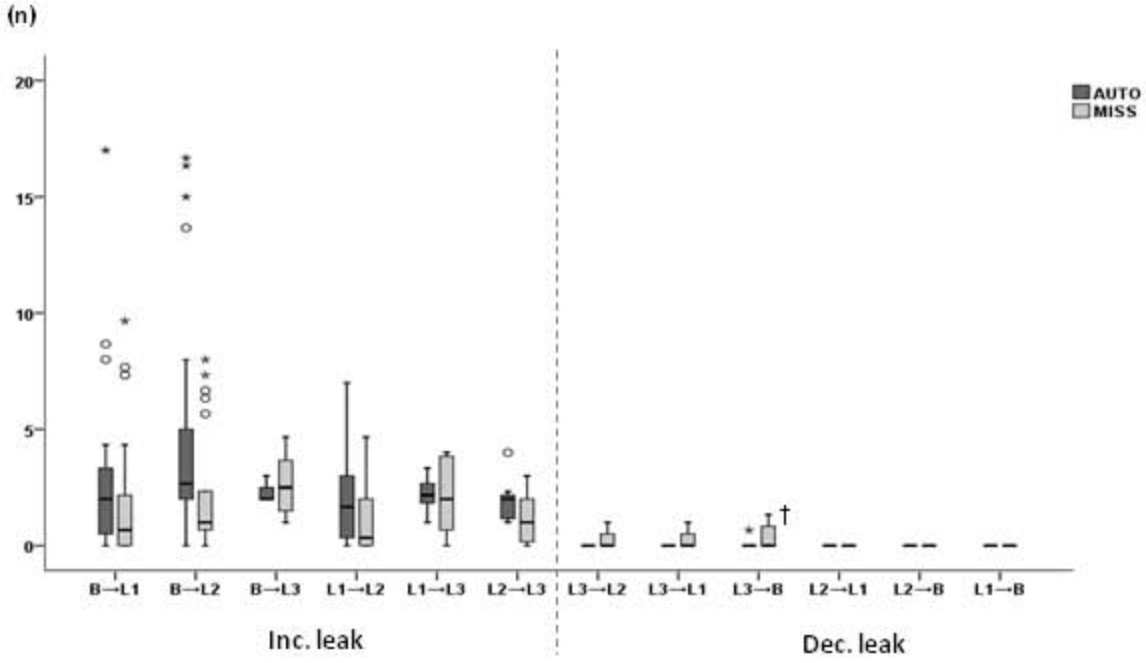
(A)

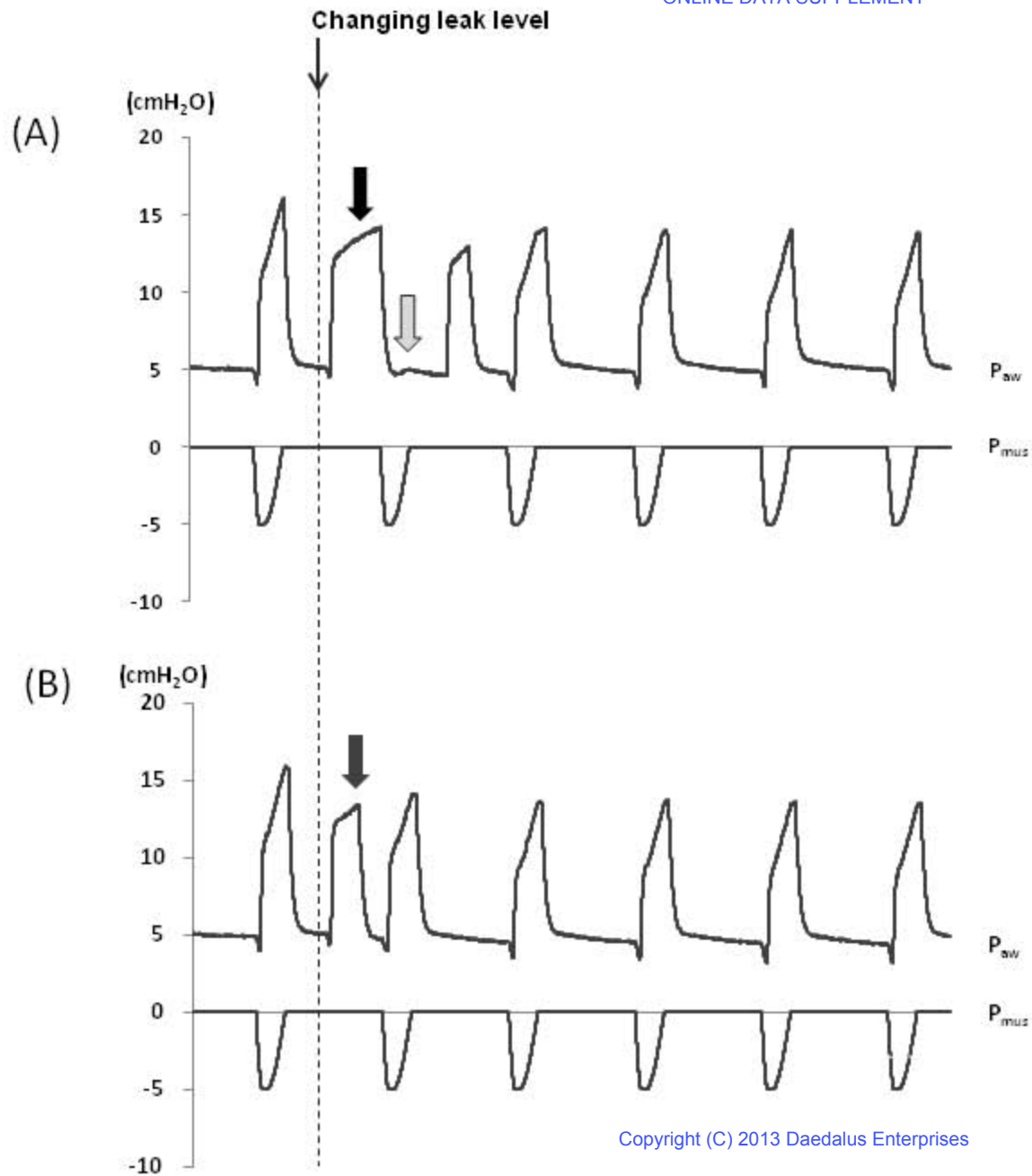


(B)

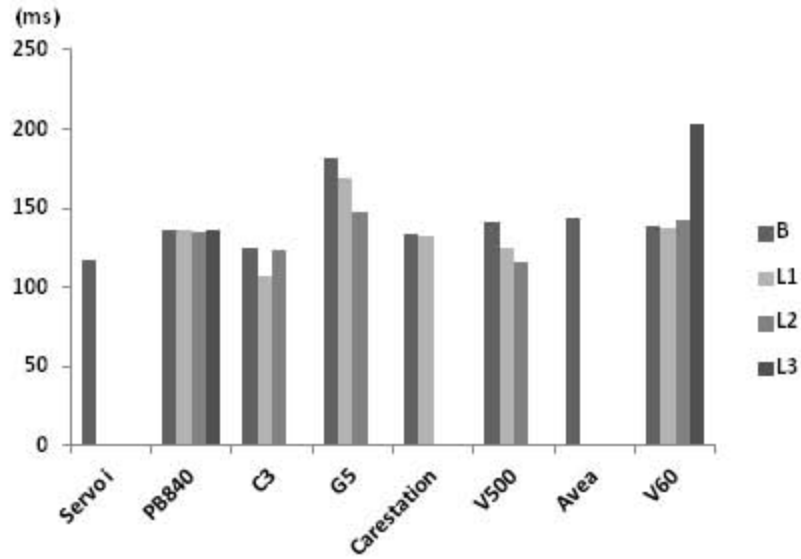


Pressure assist/control ventilation





Invasive mode (PAC) COPD model



Invasive mode (PAC) ARDS model

